Journal of the Korean Nuclear Society
Volume 4, Number 4, December, 1972

≪Original≫ Experimental Determination of Differential Fast Neutron Spectra in a Reactor using Threshlod Detectors

Dong Hoon Kim

Reactor Engineering Division, Atomic Energy Research Institute, Seoul, Korea
(Received August 29, 1972)

Abstract

The differential fast neutron spectra above 0.5 Mev at particular spatial positions in the reactor(TRIGA MARK-II) core has been determined experimentally using several threshold activation detectors. The series expansion technique utilizing the concept of least squares optimization was used to obtain an approximate solution to the set of integral equations which are defined by the experimentally determined activation data. The influence of use of different weighting functions in the solution was analyzed in each measurement. To carry out the necessary mathematical calculations, a computer code for the UNIVAC 1106 digital computer has been prepared. Good agreement was achieved between the differential fast neutron spectra determined in this work and the computed flux determined independently using space-independent multigroup transport theory.

요 약

원자로(TRIGA MARK-Ⅱ)노심의 특정위치에서 0.5 Mev 이상의 고속중성자 스펙트럼을 발단검출기(Threshold detector)를 사용하여 실험적으로 측정하였다.

발단검출기의 실험적인 방사화자료로서 결정되는 일련의 적분방정식에 대한 근사해를 얻기 위하여 최소자승법의 개념을 이용한 급수전개법을 사용 하였다. 상이한 가중함수 (weighting function)를 사용 하므로서 해답에 미치는 영향을 각측정에서 분석 검토 하였다.

이방법의 사용에 관련되는 수치계산을 수행하기 위하여 UNIVAC 1106전자계산기를 위한 계산코드를 준비하였다. 본 연구에서 얻은 미분적 고속중성자 스펙트럼은 독립적으로 다군 수송이론에 의하여 얻은 결과와 잘 일치하였다.

1. Introduction

The purpose of this work was to determine experimentally the energy dependence of the fast(>0.5Mev) differential neutron flux, $\phi(E)$, at particular spatial positions in TRIGA MARK-Ⅱ reactor. More specifically, the flux, $\phi(E)$, in the center positions of the

central thimble and the outermost fuel ring adjacent to the piercing beam tube(#1) have been calculated from irradiation measurements using several threshold activation detectors.

Threshold reactions are very useful tool in the determination of the fast neutron fluxes.

Much of the early works[1),2)] in this field have been devoted primarily to determining the integral flux above some specified threshold energy, ϕ_{Ei}, where

$$\phi_{Ei}=\int_{E_i}^{\infty}\phi(E)dE \tag{1}$$

and

E_i=threshold energy of the detector.

This is accomplished by irradiating several detector whose activation cross section resemble step function and then determining the resulting activities, A_i,

$$A_i=\int_0^{\infty}\phi(E)\sigma_i(E)dE \tag{2}$$

where

$\sigma_i(E)$=microscopic activation cross section of the i^{th} detector,

A_i =activity per target atom of the i^{th} detector.

From Eq. (2), with A_i measured and $\sigma_i(E)$ known, $\phi(E)$ can be found. Eq. (2) is a linear integral equation, called a Fredholm equation of the first kind. Solution of this equation is relatively easy when the kernel, $\sigma_i(E)$, is a continuous analytic function of energy. However, $\sigma_i(E)$ is often only a set of values at discrete energies, and thus the solution becomes much more difficult.

Various methods suggested by several investigators for solving Eq. (2) will be examined in a later section.

2. Methods of Solution

The series expansion methods, which was first introduced by Uthe[3)], is used primarily in the fast range(>0.5 Mev) where the activation cross sections of most substances exhibit a threshold appearance. It requires the assumption that the differential flux can be expressed as a finite series in energy multiplied by suitably chosen weighting function.

On the other hand, the method using a series expansion of polynomial functions has been suggested independently by Trice[4)] and Hartman[5)]. Here the spectrum is given as a sum of polynomial functions

$$\phi(E)=W(E)\sum_{j=1}^{n}a_j\phi_j \tag{3}$$

where

$W(E)$=weighting function,

n =number of detectors,

a_j =unknown constant coefficient to be determined,

ϕ_j =expansion function.

Usually the expansion functions are selected from a complete orthonormal set[6)], but other functions have been used by some authers[3)]. However, the same mathematical procedure for determining the unknown coefficients has, in general, been followed by most of the investigators.

Substitution of Eq. (3) into each equation of a set of equations of the type illustrated by Eq. (2) leads to the following set of linear algebraic equations which may be solved for the unknown coefficients:

$$A_i=\sum_{j=1}^{n}a_jS_{ij}\quad i=1,n \tag{4}$$

where

$$S_{ij}=\int_{E_i}^{\infty}\sigma_i(E)W(E)\phi_j(E)dE \tag{5}$$

The solutions obtained by this method are not exact, and widely differing solutions can be obtained by making small changes of the input activation data. In some cases, depending on the choice of detectors and on the errors which are always present in the experimentally determined activation cross sections and activities, the solutions do not exist.

For example, if two or more detectors have very similar cross sections, then the corresponding rows of the S matrix of Eq. (5) will be quasi-proportional and the solution of the system of equations may not be obtained by the conventional matrix inversion technique. Such ill-conditioning, or instability, is further enhanced by the error in the cross sections and activities.

The least squares method has been widely used in numerical calculations in order to obtain the best approximation to an exact function with a finite number of expansion terms of polynomials. Di Cola and Rota[7),8)] first applied this method to the determination of fast neutron spectra by series expansion approximation.

Suppose that the fast differential neutron flux can be approximately represented by

$$\phi(E)\approx\phi'(E)=W(E)\sum_{j=1}^{t}a_j\phi_j(E) \qquad (6)$$

where t is the number of terms in the series expansion and is called the approximation number($t\leq n$, where n is the number of detectors). The best approximation to $\phi(E)$ is assumed to that which minimizes the following quadratic form of the relative deviation:

$$Q(t;a_1,a_2,\ldots,a_t)=\sum_{i=1}^{n}\left\{\frac{A_i-\int_{E_i}^{\infty}\sigma_i(E)\phi'(E)dE}{A_i}\right\}^2 \qquad (7)$$

in the sense of least squares. For Q to be a minimum, it is necessary that the following equations hold:

$$\frac{\partial Q}{\partial a_j}=0,\quad j=1,\ t \qquad (8)$$

This leads to the following set of linear algebraic equations ($t\times t$) in the t unknowns, $a_1,\cdots a_t$:

$$R^T\ Ra=R^T\ e. \qquad (9)$$

Therefore,

$$a=(R^TR)^{-1}R^T\ e, \qquad (10)$$

where

$$a=\begin{pmatrix}a_1\\a_2\\\vdots\\a_t\end{pmatrix},\quad e=\begin{pmatrix}1\\1\\\vdots\\1\end{pmatrix},\quad R=\begin{pmatrix}r_{11}\cdots\cdots r_{1t}\\r_{21}\\\vdots\\r_{n1}\cdots\cdots r_{nt}\end{pmatrix}$$

$$r_{ij}=\frac{S_{ij}}{A_i}=\frac{1}{A_i}\int_{E_i}^{\infty}\sigma_i(E)\,W(E)\phi_j(E)dE$$

A differential flux spectrum, ϕ'(E), may be calculated for each different value of t. The spectrum which minimizes Q is assumed to be the best fit to the experimental data in the sense of least squares.

In this method which was named as "relative deviation minimization method", it is possible, at least in principle, to use all of the available activation data even if an instability exists. For example, the spectrum calculated by this method for the case t=n−1 may be physically acceptable : whereas, the calclated spectrum for the case t=n may not be physically acceptable—in both cases, all of the experimental activation data are used.

On the other hand, in the generalized method presented previously, it would be necessary to discard some of the activation data in order to remove an instability or ill-conditioning.

This method provides a means by which the instability problem may be eliminated without rejecting reasonably good experimental data.

However, in some cases, it may be found that the interpretation of the experimental activation data by this method does not give satisfactory results for all values of t depending on the selection of detectors and the errors both in the cross section data and activation data. In order to obtain a better solution and a criterion for establishing the relative confidence in the calculated results under such conditions, the following considerations were incorporated into this method.

1) Weighting Function

In computing the fast neutron spectra by

the series expansion method, the weighting function W(E) may have an important role in solving the problem, because the expansion in Eq. (6) may be interpreted in the sense that the unknown flux is obtained from the shape of the function W(E) through the deformation described by the series expansion.

The fission neutron spectrum can be successfully represented by the following semi-empirical formula for the fission spectrum of U-235 by slow neutrons[9]

$$\phi(E)\sim exp[-E]\sinh(2E) \tag{11}$$

However, in a thermal reactor, the neutron spectra are deformed by the processes of elastic and inelastic scattering and absorption by the moderator and other structural materials. Therefore the forms of the fast neutron spectra usually deviate from the fission neutron spectral shape. In general, the reactor spectral shape may be reasonably assumed to approximately follow a function proportional to the exponential function $e^{-\beta E}$ in high energy region. Here β is a positive constant, and should be determined in each measurement.

In view of these physical arguments, we can set

$$W(E)=exp(-\beta E) \tag{12}$$

in Eq. (6). In some cases, the series expansions combined with the weighting function may not adquately represent the true spectum depending on the choice of detectors and the errors in the cross sections and the activation data, as previously indicated. The calculated spectra may exhibit instabilities for some values of β.

The existence of an instability in a neutron spectrum computed by this method becomes evident if the spectrum shows a highly oscillatory appearance in which there is an extremely large dip in the spectrum or, even worse, the flux becomes negative at one or more interior energy points. Such a spectrum is unacceptable from the physical point of view.

It is necessary, then, to find the value of β which gives the best solution to Eq. (6). In this study, an attempt was made to investigate the influence of β on the neutron spectra calculated using series expansion method with minimization of the relative deviation.

2) Statistical Error Analysis

The study of error propagation in the series expansion method was carried out by the use of a Monte Carlo technique[8),10)]

From the statistical error estimates of the experimental input data in the form

$$A_i \pm h_i A_i \text{ and } \sigma_i \pm k_i \sigma_i \quad i=1, n$$

it was possible to estimate the uncertainty in the calculated neutron spectra in the form

$$\phi_d^i(E_k) \pm S_\phi^i(E_k) \tag{13}$$

where $\phi_d^i(E_k)$ is the calculated flux at energy E_k using the mean values of the input data.

A normal error distribution was assumed for each of the 2n input data(n input data for each of activation data and cross section). Each datum was randomly varied g times and the g sets of input data were then processed to produce g different functions $\phi^i(E_k)$ for each selected discret energy E_k.

If the number g is sufficiently high, for every value of E_k, the following equation is satisfied:

$$\phi_d^i(E_k)=\bar{\phi}^i(E_k)=\frac{\sum_{\ell=1}^{g}\phi_\ell^i(E_k)}{g} \tag{14}$$

and

$$S_\varphi^i(E_k)=\left\{\frac{\sum_{\ell=1}^{g}[\bar{\phi}^i(E_k)-\phi_\ell^i(E_k)]^2}{g-1}\right\}^{\frac{1}{2}} \tag{15}$$

A FORTRAN code, FNS, for the UNIVAC 1106 has been prepared which performs the calculations presented above. Laguerre polynomials are incorporated into the code as the

series expansion functions. Here, the standard deviations in each detector cross section must be input as a constant value which is representative of the complete domain of definition of each cross section. An iterative scheme permits the β value in the weighting function to be varied in each calculation.

3. Numerical Test

In order to establish calculation methods and some degree of confidence in identifying calculated neutron spectra, numerical tests were carried out with a known neutron spectrum. A test consists of defining a flux spectrum, $\phi_T(E)$, over the energy range from 0.5 Mev to 15 Mev; then using $\phi_T(E)$ together with the evaluated cross section data to perform the integrals indicated in Eq. (2). The integrals were performed over the range from E_i to 15 Mev. The value of the upper limit was chosen as the energy above which all activations are essentially negligible, either because all cross sections are small or the flux is small. These calculations generated a fictitious set of activities, A_i, $i=1, n$. A set of A_i derived from the cross section data by a test neutron spectrum[7]:

$$\phi_T(E)=(e^{-2.3E}+0.03e^{-0.75E})e^{-\frac{1}{0.5+E}} \quad (16)$$

The five activation reactions which were utilized in this test were: $^{27}Al(n, \alpha)^{24}Na$, $^{56}Fe(n, p)^{56}Mn$, $^{58}Ni(n, p)^{58}Co$, $^{115}In(n, n')^{115*}In$, $^{54}Fe(n, p)^{54}Mn$.

Of the above reactions, the ^{115}In reaction has the lowest threshold energy, 0.41 Mev. The activation cross sections used throughout this work were taken from an extensive compilation of cross section data in Ref. 11.

The cross sections were input at discrete energies. The code is written in such a way that flux can be calculated at the discrete energies for which the cross sections are defined. Since narrow resonances are not prevalent in fast threshold cross sections(an exception is Ni, whose activation cross section exhibits narrow resonances in the region of 3 Mev), it is not necessary, in general, to have extremely fine energy resolution of the cross section data.

The activation rates A_i of each threshold detector for the test neutron spectrum expressed by Eq. (16) were calculated using Eq. (2).

1) Step, Polygonal, Polynomial Methods

Prior to performing a interpretation of these activation data by the proposed method, several other methods[12),13)] which have been used by many investigators were examined.

These methods were

a) Step-function approximation,

b) Polygonal method,

c) Polynomial expansion method

The results obtained from these calculations

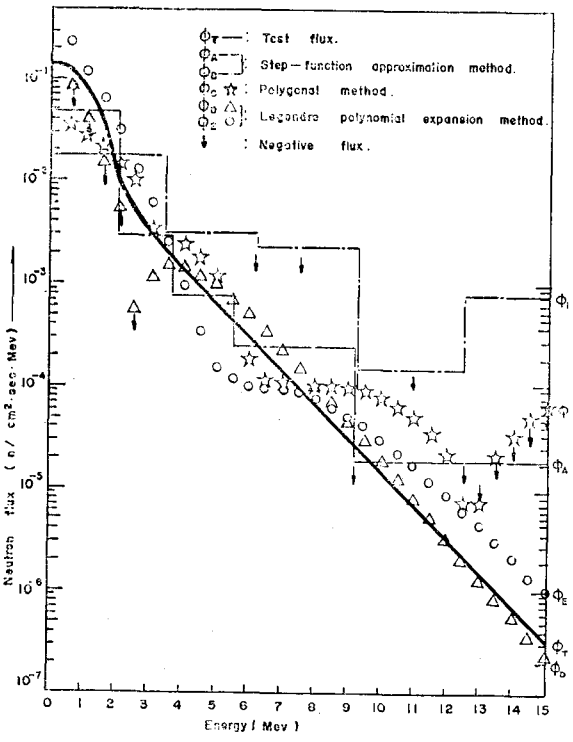

Fig. 1. Calculated fast neutron spectra for test flux

are given and compared with the true flux in Fig. 1.

The step-function approximation divides the total energy interval over which $\phi(E)$ is to be measured into n energy groups, where n is the number of detectors used, and assumes the flux in each energy group is a constant. The resulting n equations obtained from Eq. (2) by setting $\phi(E)$ constant can then be solved.

In attempting to find neutron spectra by this method, two different energy arrays were considered. These arrays were designated as A and B, and the corresponding flux spectra calculated from these arrays are shown as ϕ_A and ϕ_B in Fig. 1. Both spectra were negative in some energy bands.

In the polygonal method, it is assumed that the true neutron spectrum can be approximated by a series of values at various energy points and that between these values the flux varies linearly. This method gave a fairly good approximation to the test flux, even though negative fluxes were found in the high energy region as shown in Fig. 1. A better solution may be obtained using a certain energy array and a large number of detectors. However, the system complexity and the probability of an ill-conditioning increases.

Since the above methods provide no reliable logical method of finding suitable energy arrays, these method are not considered very accurate.

For finding the spectra by the polynomial series expansion method, the orthonormal sets of the Legendre polynomials were employed. The flux spectrum calculated using all five detectors is given as ϕ_D in Fig. 1. In the lower energy region, negative values of flux were found. Such ill-conditioning could be removed, as shown by ϕ_E, which was obtained by rejecting Ni detector.

In the set under investigation it is possible to note the energy dependence of the cross sections for ^{58}Ni and ^{54}Fe is similar. It follows that the rows of the matrix S in Eq. (4), related to these detectors, are quasi-proportional. This generates an instability that may be enhanced using error-affected activation rates.

2) Relative Deviation Minimization

The data processing by this method was carried out using the UNIVAC 1106 digital computer.

The weighting function used in this test calculation, for which the spectrum was defined by Eq. (16), has a general form of Eq. (12), in which β is a positive constant. In order to examine the influence of β on the spectra calculated by this method, value of β assumed in repeated calculations was varied from 0.5 to 1.5 in a step of 0.1.

At present, a 5% input error was taken

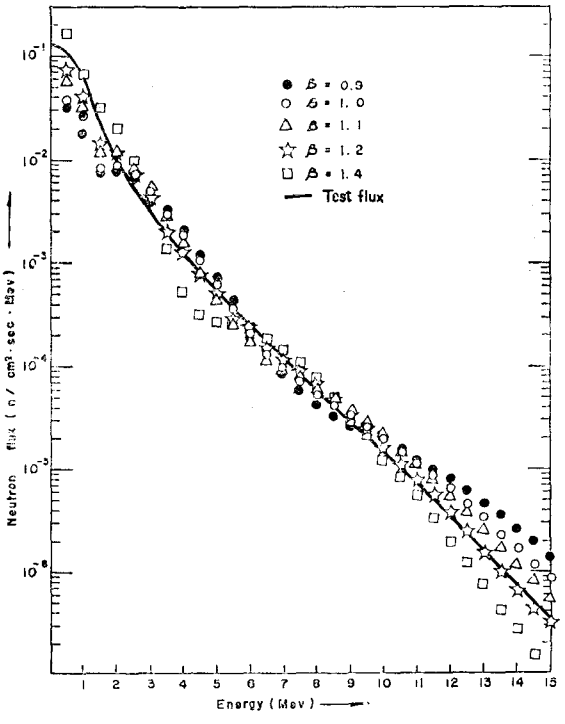

Fig. 2. Calculated fast neutron spectra for test flux with t=5

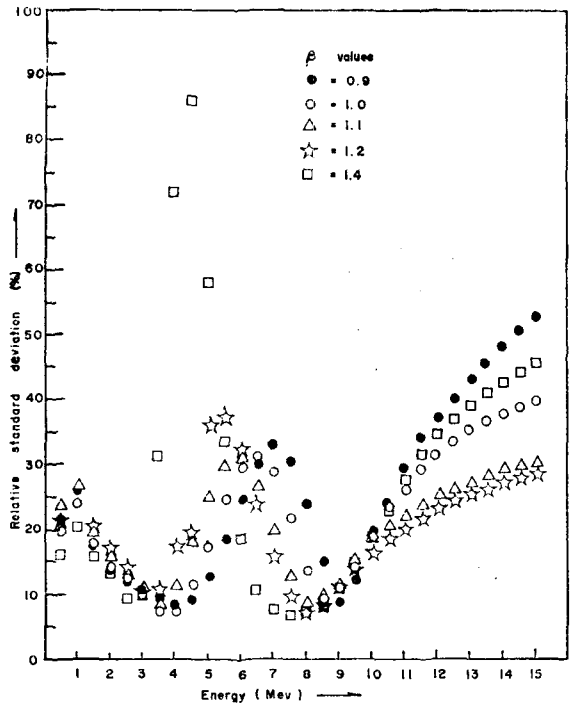

Fig. 3. Influence of the weighting function on the output error with t=5

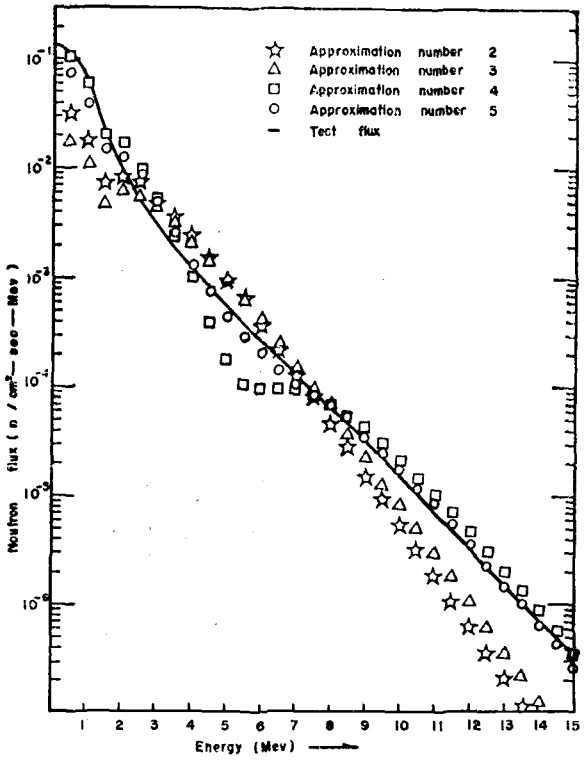

Fig. 4. Calculated fast neutron spectra for test flux with β=1.2

into account for both A_i and $\sigma_i(E)$. This assumption seems to be realistic, since activation rates in actual measurements are usually affected by a 3 to 5% error and error of 5% is typical in the cross sections[8].

The test calculations were performed using approximation numbers ranging from t=2 to t=n, where n=5, for each value of β. In all cases, 150 histories were used in the Monte Carlo calculations.

A portion of the results of these test calculations are presented in Fig. 2, 3 and 4 along with the original spectrum. As shown in Fig. 2, the influences of β values on the calculated spectra is significant, especially in high energy region. Good approximations to the true spectrum, from the standpoint of agreement with the original spectrum, were obtained in cases with β=1.1 and β=1.2 when t=5 (Fig. 4).

In fact, the relative magnitudes of the uncertainties in the calculated results, which depend on β value, are indicative of the degree of confidence in the computed spectra

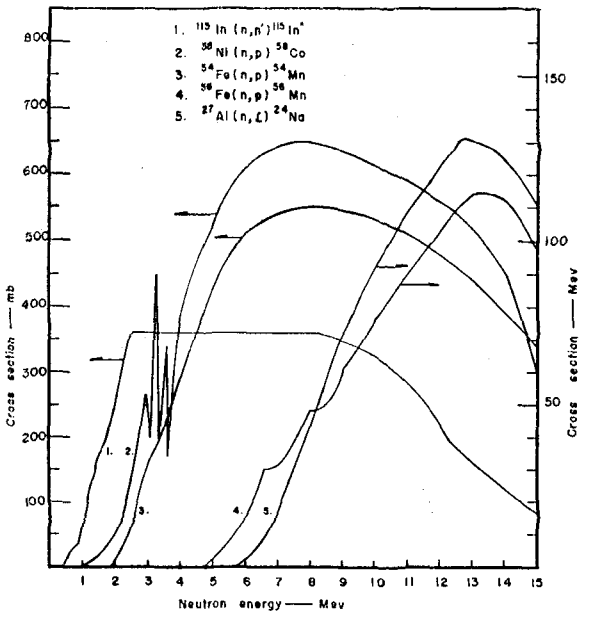

Fig. 5. Activation cross sections of threshold detectors

Comparing Fig. 2 and 3, it should be noticed that the relative standard deviations in the calculated differential spectra are large at points where the disagreement between the calculated spectral shape and the true spectral shape is also large.

The oscillating character of the error is related to the nature of the functions chosen for the series expansion(Fig. 3).

The results of these test calculation indicate that the statistical analysis of the errors could give some information about the goodness of the expansion of Eq. (6), which is combined with the weighting function as defined by Eq. (12), in the particular case under investigation.

4. Experiment

The primary activation reactions used in this experiment were: $^{115}In(n, n')^{115*}In$, $^{58}Ni(n, p)^{58}Co$, $^{54}Fe(n, p)^{54}Mn$, $^{56}Fe(n, p)^{56}Mn$, $^{27}Al(n, \alpha)^{24}Na$.

The cross section versus energy curves used in the present work are given in Fig. 5.

All of the detectors used in the experiment were in the form of metalic foils, and consisted

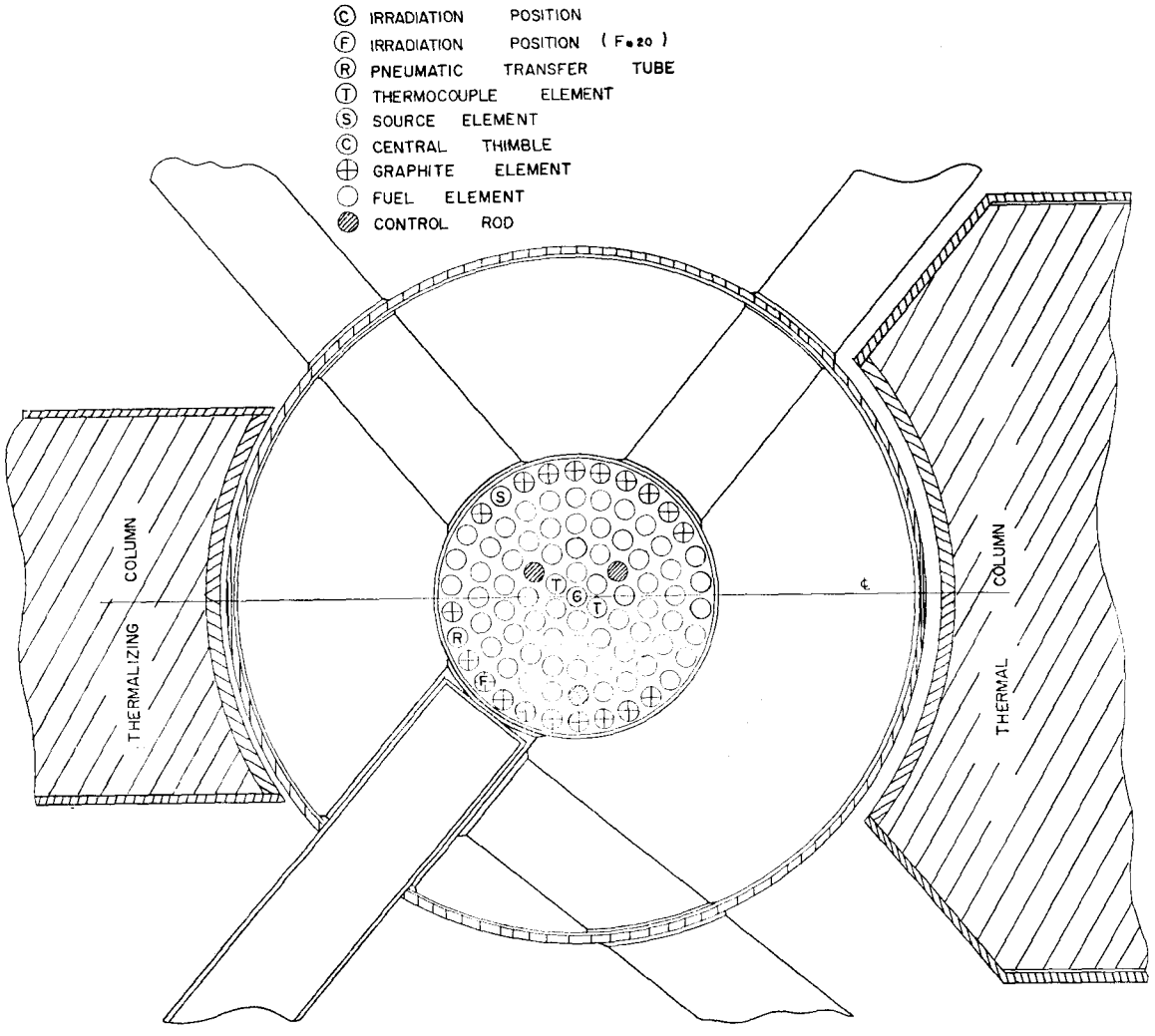

Fig. 6. Plane section of TRIGA MARK-I core

of high purity materials in order to avoid chemical separation process after irradiation. The physical characteristics of detectors are given in Table. 1.

Since several different detectors were used to determine the differential neutron flux at two spatial locations in the center position of the central thimble and in the center position of the outermost fuel hole(F-ring) adjacent to the piercing beam tube of TRIGA MARK-Ⅱ, it was required that each detector was irradiated at the position in separate runs. However, because of the large amount of

Table 1. Physical characteristics of threshold detectors

Detector	Size	Mass (mg)	Isotopic target	Target isotopic abundance (%)	Purity (%)
Ni	dia. 1 cm	39.0	Ni^{58}	67.76	99.0
Al	dia. $\frac{1}{2}$ in.	37.8	Al^{27}	100	99.986
Fe	dia. $\frac{1}{2}$ in.	139.9	Fe^{54}	5.82	98.8
Fe	dia. $\frac{1}{2}$ in.	139.9	Fe^{56}	91.66	98.8
In	dia. 0.6cm	32.45	In^{115}	95.72	99.9

reactor time required for these irradiations, it was necessary to irradiate two or three detectors simultaneously. The central thimble is located at the center of the core whereas the F-ring is close to the core periphery, as shown in Fig. 6.

All detectors were completely shielded with 0.5mm thick cadmium covers in order to reduce the production of undesirable activities by thermal neutrons. The holder assembly which contained the cadmium covered detector had a cylindrical form of 12.5cm in height and 2.5cm in diameter and was made of aluminium.

Since the TRIGA MARK-Ⅱ reactor is a pool-type water reactor, the holder could be inserted into the position from the top of the reactor. A stainless steel wire approximately 25 feet long was attached to the top of the holder in order to place it accurately at the desired position for each run.

With the holder on the top of the standpipe, the reactor power was increased from shutdown to 250KW. After the desired power level had been maintained for about ten minutes, the holder was lowered into the hole. The time required to lower the holder into proper position from the top of the standpipe was less than five seconds. Irradiation proceeded until the run was ended by simultaneously scramming the reactor and withdrawing the holder from the hole. The irradiation times for the runs ranged from 12 minutes to 1 hour, depending on the detectors in order to give adequate activation for counting.

The activity of each foil detector was counted on the gamma channel of the γ-β coincidence counting system for measuring gamma rays. Calibration of the counter in order to convert count rate to absolute activity

Table 2. Experimental data

Reaction	Half-life	Threshold energy (Mev)	Photopeak energy (Mev)	Central thimble		F-ring	
				Activation rate (per sec)	Fractional standard deviation	activation rate (per sec)	Fractional standard deviation
$Al^{27}(n, \alpha)\ Na^{24}$	15 hrs	3.26	1.38	4.44×10^{-15}	0.019	9.16×10^{-16}	0.035
$Fe^{56}(n, p)\ Mn^{56}$	2.58 hrs	2.95	1.81	8.81×10^{-15}	0.034	2.04×10^{-15}	0.037
$Fe^{54}(n, p)\ Mn^{54}$	312 days	2.40	0.84	5.00×10^{-13}	0.048	1.46×10^{-13}	0.050
$Ni^{58}(n, p)\ Co^{58}$	71 days	0.62	0.81	6.19×10^{-13}	0.026	1.50×10^{-13}	0.034
$In^{115}(n, n')\ In^{115*}$	4.4 hrs	0.41	0.334	1.72×10^{-12}	0.052	2.10×10^{-13}	0.051

was performed with calibrated standard sources, which were supplied by the IAEA Laboratory. By use of these standard sources, the efficiency of the 2″×2″ NaI (Tl) scintillation counter at each gamma-ray energy was obtained by measuring the total number of photoelectric absorptions of a particular gamma rays with fixed counting geometry. Counting losses due to the counter dead time are negligible provided the observed count rate is less than 100,000 counts per minute. Each detector was counted a minimum of two times on the counter in order to provide a check on the decay time of the isotope being counted.

The activation rates of each detector, corrected for fluctuations in power level between runs, are presented in Table 2 along with the fractional standard deviations.

5. Results and Discussions

In evaluating the standard deviations of activation data, the systematic and the statistical errors in the counting were taken into account. Corrections for the perturbation effects of self shielding and flux depression by the detectors were assumed negligible because the cross sections and the thicknesses of the detectors are quite small in the fast range.

The activation cross section data used in this work were taken from Ref. 11. The evaluated cross sections, which are based on agreement between different experimenters, competence of the experimenters, etc., are tabulated for each reaction such that linear interpolation is possible between such tabulated points. No reliable information on the representative error of each cross section over the complete domain of energy was available. However, since these values were needed as input data for the evaluation of the calculated results, 5% error was assumed reasonable for all detectors as described earlier.

The same expansion function, weighting functions and procedures were applied in this work as had previously proved to be successful for a typical reactor-type fast neutron spectrum in numerical tests.

It was found that, although the results are not shown herein, the uncertainties and the shapes of the calculated fast neutron spectra for all values of β were most reasonable with $t=4$ among other values of t.

The uncertainties associated with each value of neutron flux at the central thimble are presented in Fig. 7. The cal culated fast neutron spectral shapes at this position were plotted for several values of β in Fig. 8.

As indicated in Fig. 8, there are large dips at 1 Mev in cases of $\beta=1.0$ and $\beta=1.1$, and negative fluxes at the energy points of 0.5 and 1.0 Mev when $\beta=1.0$, which is not acceptable from a physical point of view. However, this does not imply that the remaining portion of spectra are unacceptable.

The results for the central thimble were compared with the spectrum[14] calculated using the multigroup transport code, GAM-1[15]. GAM-1, which has been used for designing TRIGA reactors, by which generates fast neutron cross sections for the desired group structure by solution of the P1 equations from which a space-independent flux is derived.

It should be noted that the energy region of underswings of the calculated flux with respect to GAM-1 spectrum between 4 and 7 Mev are corresponds to the points which the uncertainties are large as shown in Fig. 7.

For F-ring, the results of the calculation are reported in Fig. 9 and 10.

The oscillatory appearance and negative fluxes in some of the results were found depending on approximation numbers and β values. It was observed that the uncertainties associated with such ill-conditioned flux

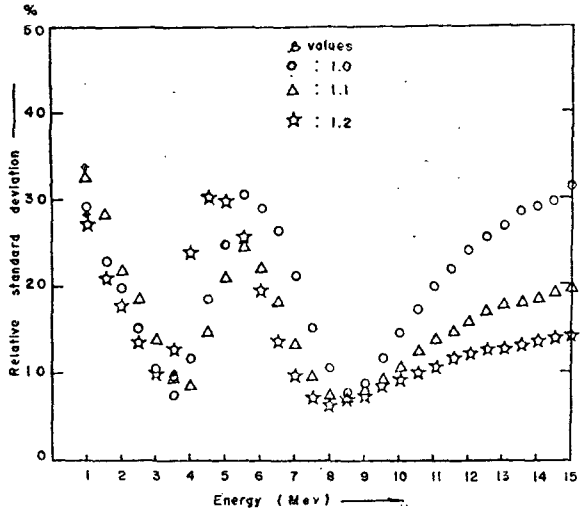

Fig. 7. Influence of β on standard deviation of fast neutron spectra at central thimble, t=4

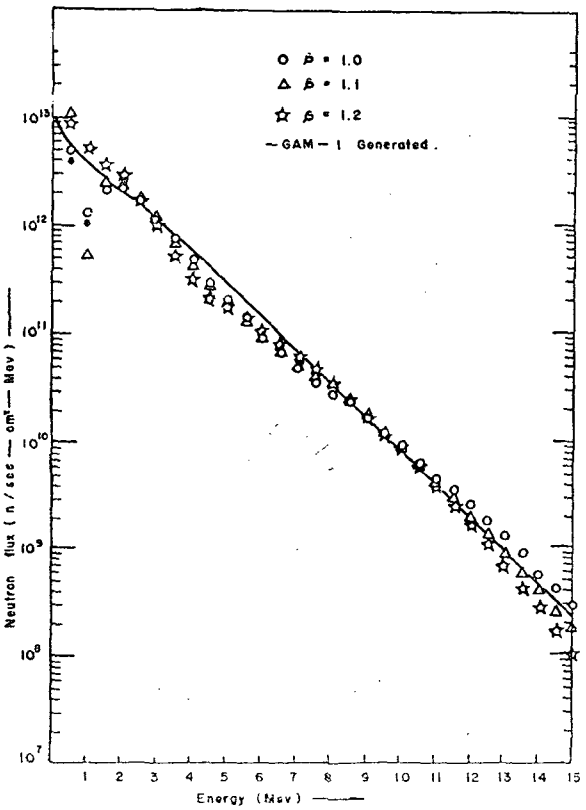

Fig. 8. Fast neutron spectra at central thimble, t=4

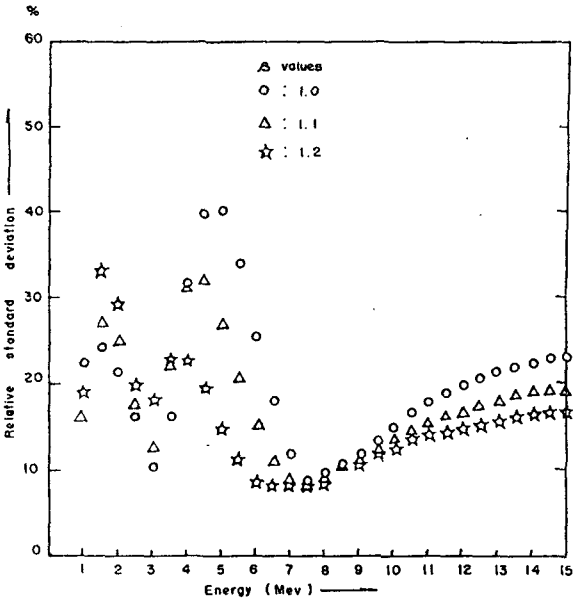

Fig. 9. Influence of β on standard deviation of fast neutron spectra at F-ring, t=4

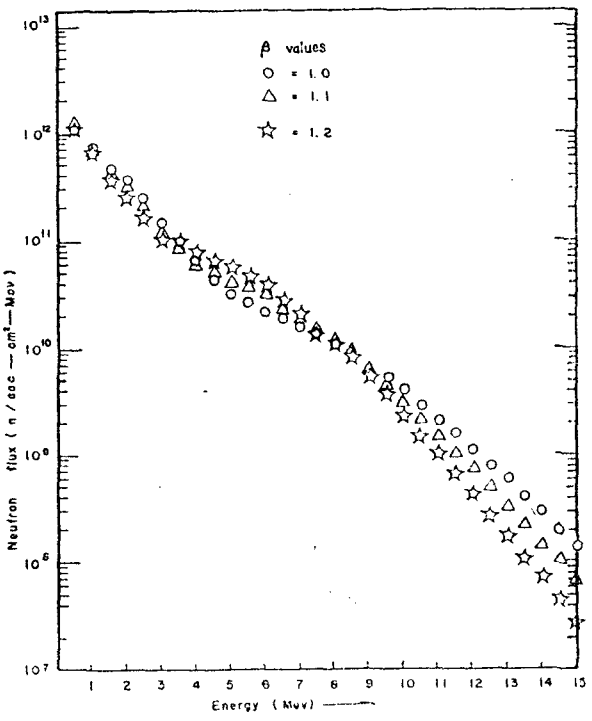

Fig. 10. Fast neutron spectra at F-ring, t=4

Table 3. Calculated results with t=4 and β=1.2 for the central thimble

E (Mev)	Neutron flux (n/sec-cm²-Mev)		Standard deviation	
	Calculated	Monte carlo	Absolute	Relative
0.50	1.79×10^{13}	1.80×10^{13}	4.34×10^{12}	0.240
1.00	5.51×10^{12}	5.58×10^{12}	1.53×10^{11}	0.275
1.50	3.81×10^{12}	3.81×10^{12}	7.95×10^{11}	0.207
2.00	3.10×10^{12}	3.13×10^{12}	5.67×10^{11}	0.181
2.50	1.91×10^{12}	1.93×10^{12}	2.71×10^{11}	0.141
3.00	1.05×10^{12}	1.06×10^{12}	1.06×10^{11}	0.099
3.50	5.69×10^{11}	5.75×10^{11}	7.77×10^{10}	0.135
4.00	3.27×10^{11}	3.29×10^{11}	7.79×10^{10}	0.236
4 50	$2\ 12\times10^{11}$	$2\ 13\times10^{11}$	6.52×10^{10}	0.306
5.00	1.55×10^{11}	1.56×10^{11}	4.75×10^{10}	0.305
5.50	1.22×10^{11}	1.23×10^{11}	3.13×10^{10}	0.256
6.00	9.85×10^{10}	9.87×10^{10}	1.92×10^{10}	0.194
6.50	$7\ 86\times10^{10}$	7.87×10^{10}	1.10×10^{10}	0.140
7.00	6.13×10^{10}	$6\ 14\times10^{10}$	6.15×10^{9}	0.100
7.50	4.66×10^{10}	4.67×10^{10}	3.53×10^{9}	0.076
8.00	3.45×10^{10}	3.46×10^{10}	2.32×10^{9}	0.067
8.50	2.50×10^{10}	2.50×10^{10}	1.73×10^{9}	0.069
9.00	1.77×10^{10}	1.77×10^{10}	1.36×10^{9}	0.077
9.50	1.23×10^{10}	1.23×10^{10}	1.06×10^{9}	0.086
10.00	8.42×10^{9}	8.45×10^{10}	8.01×10^{8}	0.095
10.50	5.68×10^{9}	5.70×10^{9}	5.87×10^{8}	0.103
11.00	3.78×10^{9}	3.80×10^{9}	4.19×10^{8}	0.110
11.50	2.49×10^{9}	2.50×10^{9}	2.92×10^{8}	0.117
12.00	1.62×10^{9}	1.63×10^{9}	2.00×10^{8}	0.122
12.50	1.05×10^{9}	1.05×10^{9}	1.34×10^{8}	0.128
13.00	6.72×10^{8}	6.75×10^{8}	8.91×10^{7}	0.132
13.50	4.27×10^{8}	4.29×10^{8}	5.84×10^{7}	0.136
14.00	2.70×10^{8}	2.71×10^{8}	3.79×10^{7}	0.140
14.50	1.69×10^{8}	1.70×10^{8}	2.43×10^{7}	0.143
15.00	1.06×10^{8}	1.06×10^{8}	1.55×10^{7}	0.148

Table 4. Calculated results with t=4 and β=1.2 for F-ring

E (Mev)	Neutron flux (n/sec-cm²-Mev)		Standard deviation	
	Calcnlated	Monte Carlo	Absolute	Relative
0 50	1.23×10^{12}	1.24×10^{12}	7.11×10^{11}	0.574
1.00	6.84×10^{11}	6.89×10^{11}	1.32×10^{11}	0.193
1.50	3.82×10^{11}	3.87×10^{11}	1.28×10^{11}	0.332
2.00	2.69×10^{11}	2.73×10^{11}	$8\ 03\times10^{10}$	0.294
2.50	1.69×10^{11}	1.71×10^{11}	3.43×10^{10}	0.200
3.00	1.16×10^{11}	1.17×10^{11}	2.12×10^{10}	0.181
3.50	9.18×10^{10}	9.28×10^{10}	2.15×10^{10}	0.232
4.00	7.98×10^{10}	8.05×10^{10}	1.86×10^{10}	0.231
4.50	7.04×10^{10}	7.09×10^{10}	1.38×10^{10}	0.195
5.00	6.06×10^{10}	6.10×10^{10}	9.29×10^{9}	0.152
5.50	5.02×10^{10}	5.05×10^{10}	5.92×10^{9}	0.117
6.00	4.00×10^{10}	4.02×10^{10}	3.79×10^{9}	0.094
6.50	3.08×10^{10}	3.09×10^{10}	2.58×10^{9}	0.083
7.00	2.30×10^{10}	2.31×10^{10}	1.91×10^{9}	0.083
7.50	1.67×10^{10}	1.68×10^{10}	1.48×10^{9}	0.088
8.00	1.19×10^{10}	1.19×10^{10}	1.14×10^{9}	0.096
8.50	$8\ 29\times10^{9}$	8.33×10^{10}	8.68×10^{8}	0.104
9.00	5.68×10^{9}	5.71×10^{9}	6.42×10^{8}	0.113
9.50	3.84×10^{9}	3.85×10^{9}	4.64×10^{8}	0.120
10.00	2.56×10^{9}	2.57×10^{9}	3.27×10^{8}	0.127
10.50	1.68×10^{9}	1.69×10^{9}	2.27×10^{8}	0.134
11.00	1.10×10^{9}	1.10×10^{9}	1.54×10^{8}	0.140
11.50	7.10×10^{8}	7.14×10^{8}	1.04×10^{8}	0.145
12.00	4.55×10^{8}	4.57×10^{8}	6.86×10^{7}	0.150
12.50	2.89×10^{8}	2.91×10^{8}	4.49×10^{7}	0.154
13.00	1.83×10^{8}	1.84×10^{8}	2.91×10^{7}	0.158
13.50	1.15×10^{8}	1.15×10^{8}	1.87×10^{7}	0.162
14.00	7.17×10^{7}	7.20×10^{7}	1.19×10^{7}	0.166
14.50	4.45×10^{7}	4.47×10^{7}	7.54×10^{6}	0.169
15.00	2.75×10^{7}	2.76×10^{7}	4.74×10^{6}	0.172

values, in general, were much larger than the uncertainties for the remaining portion of the spectrum. In some cases, the negative flux values could be assumed to be actually positive values. For the results presented herein which are non-oscillatory in appearance, the uncertainties are largest at the region of 5 Mev where large scatters were observed

depending on β values.

No attempt was made to compare the calculated spectra for the F-ring location with the GAM-1 spectrum, which does not give a very accurate representation of the flux for positions near a beam tube.

As may be observed from the results for any one of two cases, i.e., the central thimble and F-ring, the spectra essentially coincide, especially when the uncertainties are considered(excluding points where large dips are observed).

If a selection of one spectrum must be made for each of two cases, the choice is obvious for both cases——namely, the spectrum calculated for t=4 and β=1.2. The primary reason for selecting the spectra calculated for t=4 and β=1.2 is that the uncertainties for the spectra calculated with these values are considerably less than the uncertainties for the spectra which are calculated using other approximation numbers and β values.

The results calculated with t=4 and β=1.2 for the central thimble and F-ring, which are plotted in Fig. 8 and 10, are given in Table 3 and 4, respectively.

6. Conclusion

The relative deviation minimization method in the calculation of differential fast neutron spectra from threshold detector activation data gave better solutions than other methods as described in the numerical test.

In the calculation by this method, the weighting function plays an important role in solution of the problem, and therefore, the choice of a suitable weighting function should be considered in each case under investigation. The weighting function of a form expressed by Eq. (12) was proven to be suitable for representing reactor-type fast neutron spectra.

It was indicated that the statistical analysis of the errors could give some information about the goodness of spectra calculated from the experimental activation data.

Using the experimental data for five detectors listed in Table 2, the reasonably good results were obtained with four terms in the polynomial expression for the flux (*i.e.*, with t=4) and with the exponential index of 1.2 (*i.e.*, with β=1.2) in the weighting function.

It should be noted that good agreement was achieved between the fast neutron spectrum obtained from the multigroup transport calculation and the calculated spectra in this work.

Acknowledgements

The auther wishes to express appreciation to Professors B. Y. Pac, H. I. Bak and C. H. Chung for their many useful suggestions and discussion throughout this work. The auther is also grateful to Mr. J. C. Yang and S. C. Oh who contributed to computer work.

References

1) Hughes, D. J., Pile Neutron Research, Chapter 4, Addison-Wesley Publishing Co. (1953)
2) Trice, J. B., Measuring Reactor Spectra with Thresholds and Resonances, Nucleonics **16**, 7(1958)
3) Uthe, P. M., Attainment of Neutron Flux Spectra from Foil Activations, USAFIT-TR-57-3 (1957)
4) Trice, J. B., Preliminary Report of an Analytical Method for Measuring Neutron Spectra, APRX-408 (1957)
5) Hartmann, S. R., A Method for Determining Neutron Flux Spectra from Activation Measurements, WADC-TR-57-375 (1957)
6) Brownell, G. L., *et al*, Neutron Spectroscopy and Dosimetry at the Medical-Therapy Facility of the MIT Reactor, Neutron Dosimetry, Vol. 1 (IAEA, Vienna, 1963) 51-70
7) Di Cola, G. and A. Rota, Analysis and Development of the Series Expansion Methods in

Threshold Detector Activation Deta Handling, EUR 588. C (1964)

8) Di Cola, G. and A. Rota, Calculation of Differential Fast-Neutron Spectra from Threshold-Foil Activation Data by Least-Squares Series Expansion Methods, Nucl. Sci. Eng. :**23**, 344-353 (1965)

9) Watt, B.E., Phys. Rev. **87**, 1034 (1952)

10) Clark, Jr., M, and K.F. Hansen, Numerical Methods of Reactor Analysis, Chapter VI, Academic Press (1964)

11) Goldberg, M.D., *et al*, Neutron Cross Sections, BNL-325, Second Edition, Supplement No. 2 (1966)

12) Fisher, G.J., Neutron Spectrum Measurements in Unmoderated Assemblies, Nucl. Sci. Eng. : **7**, 355 (1960)

13) Ringle, J. C., A Technique for Measuring Neutron Spectra in the Range 2.5 to 30 Mev Using Threshold Detectors(Thesis), UCRL-10732 (1963)

14) West, G.B., Calculated Fluxes and Cross Sections for TRIGA Reactors, GA-4361 (1963)

15) Joanou, G.D., and J.S. Dudek, GAM-1:A consistent P_1 Multigroup Code for the Calculation of Fast Neutron Spectra and Multigroup constants, GA-1850 (1961)